Original Article

Triptolide inhibits epithelial-mesenchymal transition phenotype through the p70S6k/GSK3/β-catenin signaling pathway in taxol-resistant human lung adenocarcinoma

Yu Tian[1]^, Peiwei Li[2], Zhaohua Xiao[1], Jie Zhou[1], Xia Xue[3,4], Ning Jiang[1,4], Chuanliang Peng[1,4], Licun Wu[4,5], Hui Tian[6], Helmut Popper[7], Mau-Ern Poh[8], Fabrizio Marcucci[9], Chengke Zhang[1,4], Xiaogang Zhao[1,4]

[1]Department of Thoracic Surgery, The Second Hospital, Cheeloo College of Medicine, Shandong University, Jinan, China; [2]Institute of Medical Sciences, The Second Hospital, Cheeloo College of Medicine, Shandong University, Jinan, China; [3]Department of Pharmacy, The Second Hospital, Cheeloo College of Medicine, Shandong University, Jinan, China; [4]Key Laboratory of Thoracic Cancer, Cheeloo College of Medicine, Shandong University, Jinan, China; [5]Latner Thoracic Surgery Research Laboratories and Division of Thoracic Surgery, Toronto General Hospital, University Health Network, University of Toronto, Toronto, ON M5G 2C4, Canada; [6]Department of Thoracic Surgery, Cheeloo Hospital, Cheeloo College of Medicine, Shandong University, Jinan, China; [7]Institute of Pathology, Medical University of Graz, Graz, Austria; [8]Department of Medicine, Faculty of Medicine, University of Malaya, Kuala Lumpur, Malaysia; [9]Department of Pharmacological and Biomolecular Sciences, University of Milan, via Trentacoste 2, Milan, Italy

Contributions: (I) Conception and design: Y Tian, C Zhang, X Zhao; (II) Administrative support: X Xue, L Wu, H Tian, X Zhao; (III) Provision of study materials and patients: P Li, X Xue, N Jiang, C Peng; (IV) Data collection and assembly: Y Tian, P Li, Z Xiao, J Zhou, C Zhang; (V) Data analysis and interpretation: Y Tian, C Zhang, X Zhao; (VI) Manuscript writing: All authors; (VII) Final approval of manuscript: All authors.

Correspondence to: Dr. Xiaogang Zhao; Dr. Chengke Zhang. Department of Thoracic Surgery, The Second Hospital, Cheeloo College of Medicine, Shandong University, Jinan 250033, China. Email: zhaoxiaogang@sdu.edu.cn; chengkezhang@gmail.com.

Background: Chemotherapy is one of the primary treatments for both small cell lung cancer (SCLC) and non-small cell lung cancer (NSCLC), however, chemoresistance develops over time and is a bottleneck to effective chemotherapy worldwide. Therefore, the development of new potent therapeutic agents to overcome chemoresistance is of utmost importance. Triptolide is a natural component extracted from Tripterygium Wilfordii, a Chinese plant; our study aimed to evaluate its anti-tumor effects in taxol-resistant human lung adenocarcinoma and investigate its molecular mechanisms of chemoresistance.

Methods: Triptolide's inhibition of cell viability was detected by sulforhodamine B (SRB) assay. Cell cycle was measured by flow cytometry and cell apoptosis was assessed by flow cytometry and western blot. Expression of β-catenin was analyzed by western blot and immunofluorescence (IF). The anti-tumor effects of triptolide were determined using a subcutaneous in-vivo model. Cell proliferation and apoptosis were evaluated by immunohistochemistry (IHC) and terminal deoxynucleotidyl transferase dUTP nick-end labeling (TUNEL) assay, respectively. The expression level of p-p70S6K and p-GSK-3α/β was evaluated by western blot and IHC.

Results: Triptolide inhibited cell proliferation, induced S-phase cell cycle arrest and apoptosis in taxol-resistant A549 (A549/TaxR) cells. Moreover, intraperitoneal injection of triptolide resulted in a significant delay of tumor growth without obvious systemic toxicity in mice. Additionally, triptolide reversed epithelial-mesenchymal transition (EMT) through repression of the p70S6K/GSK3/β-catenin signaling pathway.

Conclusions: Our study provides evidence that triptolide can reverse EMT in taxol-resistant lung adenocarcinoma cells and impairs tumor growth by inhibiting the p70S6K/GSK3/β-catenin pathway, indicating that triptolide has potential to be used as a new therapeutic agent for taxol-resistant lung adenocarcinoma.

^ ORCID: 0000-0001-5652-0804.

Keywords: Lung adenocarcinoma; triptolide; chemoresistance; epithelial-mesenchymal transition (EMT); Wnt

Submitted Nov 25, 2020. Accepted for publication Feb 24, 2021.
doi: 10.21037/tlcr-21-145
View this article at: http://dx.doi.org/10.21037/tlcr-21-145

Introduction

Lung cancer is the leading killer among cancers world-wide (1,2); about 85% of lung cancers are classified as non-small cell lung cancer (NSCLC) (3), and adenocarcinoma being the leading entity therein. Treatment for NSCLC includes tyrosine kinase inhibition for those with driver mutations, surgery, radiation, chemotherapy, immunotherapy, and/or a combination of these treatments. However, development of chemoresistance is one of the main challenges of chemotherapy; therefore, new drugs that can prevent or overcome chemoresistance are urgently required.

Taxol is frequently applied in NSCLC treatment. It is a microtubule-stabilizing agent, which promotes microtubule assembly, prevents depolymerization, and inhibits cell division. Despite its success as an anti-tumor drug, cancer cells gradually develop resistance to taxol, which limits its long-term effects. Many mechanisms can cause taxol-resistance: multidrug-resistant phenotype mediated by ATP-binding cassette (ABC) transporters is the best known mechanisms (4); epithelial-to-mesenchymal transition (EMT) is another mechanism for induction of resistance to chemotherapy (5,6). In EMT, epithelial cells acquire a mesenchymal phenotype, which increases their motility and promotes the establishment of metastases. Studies have shown that signaling pathways which inhibit EMT also suppress drug resistance in NSCLC (7). Therefore, molecules that target EMT signaling pathways leading to EMT inhibition or reversal, may be used to effectively overcome drug resistance in tumors.

Triptolide, a natural product extracted from Tripterygium Wilfordii, has been used to treat autoimmune diseases and inflammation in traditional Chinese medicine for years. Previous studies have revealed that triptolide exerts remarkable anti-tumor effects in many kinds of cancers, such as breast cancer (8), lung cancer (9,10), prostate cancer (11), osteosarcoma (12), neuroblastoma (13), lymphoma (14), malignant mesothelioma (15), gastrointestinal cancers (16-20), and leukemia (21). On the basis of these preclinical observations, clinical trials with this molecule are currently underway (22). However, whether and how triptolide exerts anti-tumor effects in taxol-resistant NSCLC still remains unknown.

This study aimed to identify the anti-tumor effects of triptolide in taxol-resistant lung adenocarcinoma cells, and detect related targets and signaling pathways in A549/TaxR cells. And to our knowledge, it is the first study to investigate triptolide's effect on EMT in taxol-resistant lung adenocarcinoma cells and related mechanisms worldwide.

We present the following article in accordance with the ARRIVE reporting checklist (available at http://dx.doi.org/10.21037/tlcr-21-145).

Methods

Reagents

Triptolide and taxol were obtained from AbMole Bioscience (Houston, TX, USA). Roswell Park Memorial Institute (RPMI)-1640 medium, fetal bovine serum (FBS), penicillin-streptomycin, trypsin, and other reagents related to cell culture were all purchased from Thermo Fisher Scientific, Inc. (Waltham, MA, USA).

Cell culture

The A549/TaxR cells were purchased from KeyGen Biotech (Nanjing, Jiangsu, China), while A549 cells were purchased from the Cell Bank of Chinese Academy of Sciences (Shanghai, China). Both A549 and A549/TaxR cells were cultivated by RPMI-1640 medium containing 10% FBS and 100 μg/mL of penicillin-streptomycin. To maintain resistance, taxol (70 nM) was added into the medium with A549/TaxR cells, and all cells were cultivated in 5% CO_2 under 37 ℃ conditions.

Sulforhodamine B (SRB) assay

A SRB assay was performed to detect the inhibitory effects of triptolide (23,24). Briefly, 4,000 cells were cultivated in a 96-well flat-bottom plate (NEST, Wuxi, Jiangsu, China) and incubated for 24 hours at 37 ℃, and were then

treated with triptolide (0, 20, 40, and 60 nM) for another 72 hours. The percentage of cell growth inhibition was calculated using the formula: 100% – $OD_{sample}/OD_{control}$, and IC50 values were derived by curve-fitting methods using GraphPad Prism 8 software (La Jolla, CA, USA).

Cell cycle analysis

Cells were first treated with triptolide (0, 20, 40, and 60 nM) for 24 hours, they were then harvested by trypsin, washed twice in phosphate buffered saline (PBS), and fixed in 70% ethanol at –20 ℃ for several hours. Then, the cells were suspended in PBS which contained 10 μg/mL of propidium iodide (PI) (Elabscience, Wuhan, Hubei, China) and 10 μg/mL of ribonuclease (RNase) A (Elabscience) at 37 ℃ for 30 minutes. The cell cycle was then analyzed by Beckman CytoFLEX flow cytometer (Beckman Coulter Life Sciences, Indianapolis, IN, USA) with CytExpert Software (version 2.3.1.22, Beckman Coulter).

Cell apoptosis analysis

Annexin V-FITC/PI Apoptosis Detection Kit (Elabscience) was used to detect cell apoptosis. Briefly, cells were cultivated in a 6-well plate (2×10^5 cells/well), incubated for 24 hours at 37 ℃, and then treated with triptolide (0, 20, 40, and 60 nM) for 24 hours. After cell dissociation, the cells were collected and washed twice in cold PBS, and subjected to annexin V-propidium iodide (AV-PI) double staining according to the manufacturer's instructions. Apoptosis was analyzed using the Beckman CytoFLEX flow cytometer with CytExpert Software.

Protein extraction and western blot

Primary antibodies against BAX, Caspase 3, Cleaved-Caspase 3, PARP, p-Gsk-3α (Ser21), p-Gsk-3β (Ser9), Jagged1, c-Myc, Slug, TCF8/ZEB1, p70S6K/p-p70S6K (Thr389), and Histone H3 were obtained from Cell Signaling Technology (Beverly, MA, USA); β-actin and E-cadherin were obtained from Proteintech (Wuhan, Hubei, China); β-catenin, CCND3, and HES1 were purchased from ABcolnal (Wuhan, Hubei, China); and Bcl-2, Gsk-3β, and Gsk-3α were purchased from Abcam (Cambridge, MA, USA).

The cells were analysed by an extraction buffer (cat. no. FNN0011; Thermo Fisher Scientific, Inc.) containing protease inhibitor (cat. no. 78438; Thermo Fisher Scientific, Inc.), phosphatase inhibitor (cat. no. 4906845001; Roche Diagnostics, Basel, Switzerland), and phenylmethylsulfonyl fluoride (1 mM). The concentrations of lysates were then determined by bicinchoninic (BCA) assay. We then added 20 μg of each protein sample into 10% sodium dodecyl sulfate polyacrylamide gel electrophoresis (SDS/PAGE) gels and transferred them electrophoretically onto polyvinylidene fluoride (PVDF) membranes (0.45 μm, Millipore, Bedford, MA, USA). Membranes were then incubated with the primary antibodies overnight, washed three times with 1× tris-buffered saline with Tween 20 (TBST), and incubated with horseradish peroxidase (HRP)-conjugated secondary antibodies (1:5,000, cat. no. 7074 and 7076; Cell Signaling Technology). Luminata™ Forte Western HRP substrate (Millipore) was then used to visualize the band according to manufacturer's protocol, and ImageJ 1.51 software (National Institutes of Health, Bethesda, MD, USA) was used to calculate band intensity.

Preparation of cytoplasmic and nuclear extractions for western blot analysis

The A549/TaxR cells were trypsinized after treatment with triptolide, and we then used NE-PER® Nuclear and Cytoplasmic Extraction reagents (Thermo Fisher Scientific, Inc.) to extract their cytoplasmic and nuclear fractions according to the manufacturer's instructions. Next, western blot was performed with a β-catenin specific antibody, and β-actin and Histone H3 were used as loading controls of cytoplasmic and nuclear fractions, respectively.

Transwell cell migration/invasion assays

Cell migration and invasion were determined using an 8 μm diameter pore filter (NEST). Matrigel was used to coat Transwell insert membrane during the cell invasion assay, whereas it was unnecessary in the cell migration assay. Five $\times10^4$ cells were cultivated into the upper chamber and RMPI-1640 medium containing 20% FBS was added into the lower chamber. After being treated with triptolide (0, 20, 40, and 60 nM) for 24 hours, cells were fixed across the pores with paraformaldehyde and stained with crystal violet solution. The number of cells was counted by randomly selecting 3 fields in each chamber.

Tumor model in vivo

Male Bagg Albino (BALB)/c nude 6-week-old mice were

purchased from Vital River Research Animal Services (Beijing, China) and raised in a sterile environment, and experiments were performed under a project license (No. 81874396) granted by the Ethical Committee for Animal Experimentation of the Second Hospital of Shandong University, in compliance with institutional guidelines for the care and use of animals. The A549/TaxR cells (1×10^6 cells in 100 μL of PBS) were injected into each mouse subcutaneously. When tumors reached 50–100 mm^3, the mice were assigned randomly into 3 groups, and the reagents that were injected subcutanesouly every other day were as follows: (I) 100 μL of solvent [PBS/dimethyl sulfide (DMSO) =19:1]; (II) low-dose triptolide (0.4 mg/kg); (III) high-dose triptolide (0.8 mg/kg). The body weight of each mouse was measured daily to determine whether triptolide had a toxic effect, and tumor volumes were calculated according to the formula: tumor volume (mm^3) = 1/2×(tumor length) × (tumor width)^2.

Immunohistochemistry (IHC) and histological analysis

Tumor specimens were fixed in 4% paraformaldehyde, embedded in paraffin, and sectioned. Briefly, tissue sections were deparaffinized and the slides were microwaved in citrate buffer (10 mM, pH =6.0) for 20 minutes. The sections were incubated in 3% H_2O_2 to quench the activity of endogenous peroxidase. After blocking in 1.5% goat serum (Beyotime Institute of Biotechnology, Shanghai, China) for 60 minutes at room temperature, the sections were incubated with primary antibodies of PCNA, β-catenin, p-Gsk-3α, p-Gsk-3β, and p-p70S6K at 4 ℃ overnight. The next day, the sections were incubated with a secondary antibody [1:10,000, goat anti-rabbit IgG H&L (HRP), cat. no. ab205718; Abcam], developed in diaminobenzidine, and then counter-stained with hematoxylin. Finally, the sections were examined under light microscopy.

The integrated optical density (IOD), positive staining area of p-p70S6K, β-catenin, p-GSK-3α, and p-GSK-3β in tumor specimens, and the percentage of Ki67/dUTP nick end labeling (TUNEL)-positive cells among total cells were measured by Image Pro Plus 6.0 software (Media Cybernetics, Inc., Rockville, MD, USA). The average optical density (AOD) was determined based on the formula: AOD = IOD/area for semi-quantitative analysis.

Immunofluorescence (IF)

The A549/TaxR cells were cultivated onto glass coverslips in a 6-well plate (2×10^5 cells/well) and rested overnight. After treatment with triptolide for 24 hours, the cells were fixed in 4% paraformaldehyde for 30 minutes at room temperature. The slides were then permeabilized by 1% Triton X-100 in PBS for 10 minutes and blocked in 10% normal goat serum, followed by the incubation with the β-catenin primary antibody overnight. They were then washed 3 times in PBS the next day, and incubated on the coverslips with the secondary antibody at room temperature for 1 hour. Lastly, the coverslips were mounted with mounting medium containing 4',6-diamidino-2-phenylindole (DAPI) (Abcam).

TUNEL staining

The TUNEL staining was performed to detect cell apoptosis in tumor sections using a TUNEL assay kit according to the manufacturer's instructions (Promega, Madison, WI, USA) and those of a previous study (24). Permount solution was used to dehydrate and mount the stained slides, and a BX43 light microscope (Olympus Corporation, Tokyo, Japan) was used to visualize effect of the permount solution on the slides.

Statistical analysis

All experiments were repeated 3 times in this study. Data are presented as the means ± SD, and analyzed by *t*-test and one-way analysis of variance (ANOVA). Least-significant difference and Tukey's test were used to analyze multiple comparisons. A P value <0.05 was considered to have statistical significance.

Results

Triptolide inhibits proliferation, and induces S-phase arrest and apoptosis of taxol-resistant human lung adenocarcinoma cells

Taxol (70 nM) was added to the cell culture medium of A549/TaxR cells to maintain chemoresistance. As shown in *Figure 1A*, A549 cells had little expression of multidrug resistance-associated protein 1 (MRP-1) and P-glycoprotein (P-gp), whereas the expression levels of these 2 proteins were much higher in A549/TaxR cells. The IC50 value of taxol in the A549/TaxR cells was 424nM, which was more than 50 times higher than that in A549 cells (7.8 nM, *Figure 1B*).

The chemical structure of triptolide (molecular weight, 360.4 g/mol) is presented in *Figure 2A*. To evaluate whether triptolide affects cell viability, both A549 and A549/TaxR

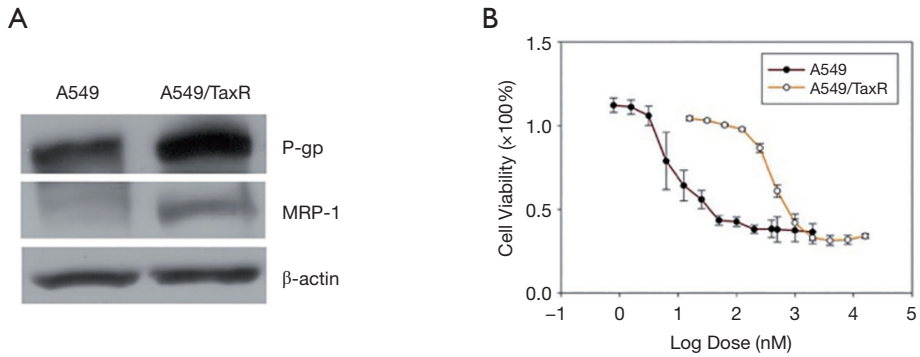

Figure 1 The effect of taxol on the proliferation of A549 and A549/TaxR cells. (A) Expression levels of MRP-1 and P-gp as determined by western blot in A549 and A549/TaxR cells. (B) Viability of A549 and A549/TaxR cells as determined by SRB assay after treatment with various concentrations of taxol for 72 hours. Cells treated by DMSO were used as a control with viability set as 100%. Each data point presents as the means ± SD. The IC50 was calculated by the Prism software. SRB, sulforhodamine B; DMSO, dimethyl sulfoxide.

cells were treated with an increasing dose of triptolide. The results indicated that proliferation of both A549 and A549/TaxR cells was inhibited by triptolide in a dose-dependent manner (*Figure 2B*, Figure S1A). Moreover, the IC50 value of triptolide in A549/TaxR cells was 15.6 nM, which was only about a half of that in the A549 cells.

The effect of triptolide exposure (20 nM, for 24 hours) on cell cycle progression was analyzed by flow cytometry in A549 and A549/TaxR cells. As shown in Figure S1B and *Figure 2C*, in the control group 36% and 51% of A549 and A549/TaxR cells were in S phase, respectively; however, the percentages rose to 49% and 77% in S phase in the group treated with triptolide. Triptolide also induced apoptosis of A549 and A549/TaxR cells. Evaluation of AV-PI positive cells revealed that at 60 nM triptolide significant apoptosis was induced in A549 cells (Figure S1C,D), A backspace is needed for the bracket and at 40 and 60 nM in A549/TaxR cells (*Figure 2D,E*). The pro-apoptotic effect was determined by western blot; increased levels of cleaved-caspase 3, cleaved-PARP, and pro-apoptotic protein BAX and decreased level of anti-apoptotic protein Bcl-2 were observed in A549/TaxR cells as shown in *Figure 2F*. In summary, triptolide inhibited proliferation, and induced S-phase arrest and apoptosis of A549 and A549/TaxR cells.

Triptolide reverses the EMT phenotype in A549/TaxR cells

A previous study indicated that triptolide can inhibit EMT in gefitinib-resistant lung cancer cells (10); therefore, we hypothesized that triptolide might suppress migration and invasion of A549/TaxR cells. The transwell-assay showed that triptolide significantly inhibited cell migration and invasion at the dosages of 20, 40, and 60 nM (*Figure 3A*). Additionally, as shown in *Figure 3B*, cell viability increased to 92% after triptolide treatment (20 nM, 24 hours). A549/TaxR cells remained viable after triptolide treatment (20 nM), apoptosis was induced (*Figure 2E*), and migration and invasion was inhibited.

The expression level of EMT markers and EMT-related transcription factors were evaluated by western blot. Epithelial marker E-cadherin was upregulated, whereas transcription factors ZEB1 and Slug were downregulated (*Figure 3C*), suggesting a reversion of the EMT phenotype in A549/TaxR cells by triptolide.

Wnt/β-catenin pathway plays a role in EMT reversion in triptolide-treated A549/TaxR cells

The canonical Wnt signaling pathway has been shown to play a role in EMT inhibition/reversion, and triptolide has been shown to inhibit the Wnt/β-catenin pathway in NSCLC cells (25,26). To test whether EMT reversion induced by triptolide was due to inhibition of the Wnt/β-catenin pathway in A549/TaxR cells, we examined the expression level of β-catenin, which together with the downstream target genes Jagged1 and c-Myc is considered the central molecule in the Wnt signaling pathway. Downregulation of β-catenin, Jagged1, and c-Myc was induced by increasing triptolide concentrations (*Figure 4A*). Since Notch can have an effect on EMT similar to that of the Wnt/β-catenin pathway (26), we evaluated the expression level of Notch1 intracellular domain (NICD1) and the downstream target genes HES1

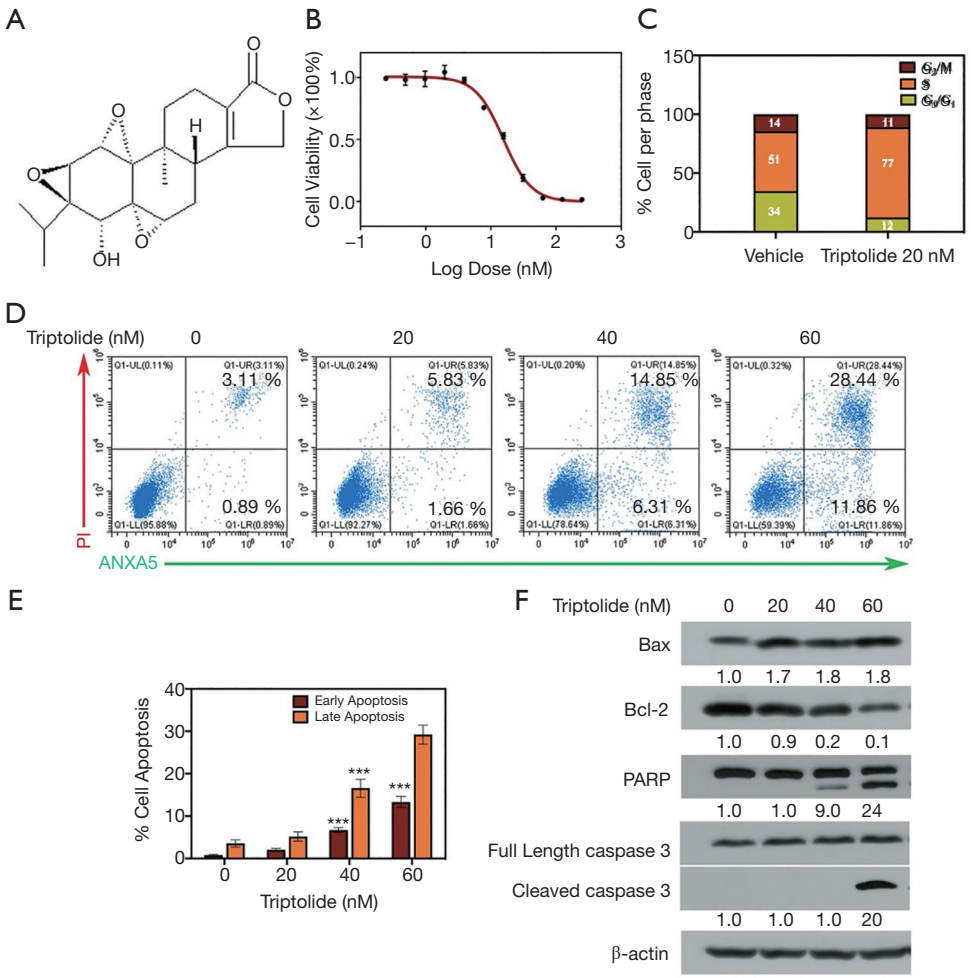

Figure 2 Triptolide inhibits proliferation and induces apoptosis of A549/TaxR cells. (A) Chemical structure of triptolide. (B) Dose-dependent inhibition of the proliferation of A549/TaxR cells by triptolide. Cell viability was determined by SRB assay after treatment with triptolide for 72 hours. (C) S-phase arrest in A549/TaxR cells after treatment with triptolide (20 nM) for 24 hours. (D) Representative flow cytometric graphs of A549/TaxR cells after treatment with triptolide (0, 20, 40, and 60 nM) for 24 hours. (E) Quantification of apoptotic cells after treatment with triptolide. The graph shows AV-PI positive cells, and the data are presented as the means ± SD. (F) Expression levels of PARP, Caspase-3, Bcl-2, and Bax in A549/TaxR cells which were detected by western blot after treatment with triptolide for 24 hours. ***P<0.001 compared to controls. SRB, sulforhodamine B; AV-PI, annexin V-propidium iodide; SD, standard deviation.

and CCND3. Our results did not show significant changes in the level of NICD1, HES1, and CCND3.

Nuclear translocation of β-catenin is critical for activation of the Wnt/β-catenin pathway. To verify whether triptolide inhibits the Wnt signaling pathway, western blot and IF were used to detect the cytoplasmic and nuclear levels of β-catenin. Both cytoplasmic and nuclear β-catenin levels were reduced by triptolide (*Figure 4B,C*), with the reduction of nuclear β-catenin being more prominent. These results allow to conclude that triptolide reversed EMT by repressing the Wnt/β-catenin signaling pathway.

Triptolide inhibits growth of A549/TaxR xenografts in vivo

A mouse model was established to investigate the effect of triptolide *in vivo*. The mean volumes of subcutaneous tumors in low-dose (0.4 mg/kg) and high-dose (0.8 mg/kg) triptolide groups were smaller than those in the vehicle group (*Figure 5A,B*). At the termination of the experiments the

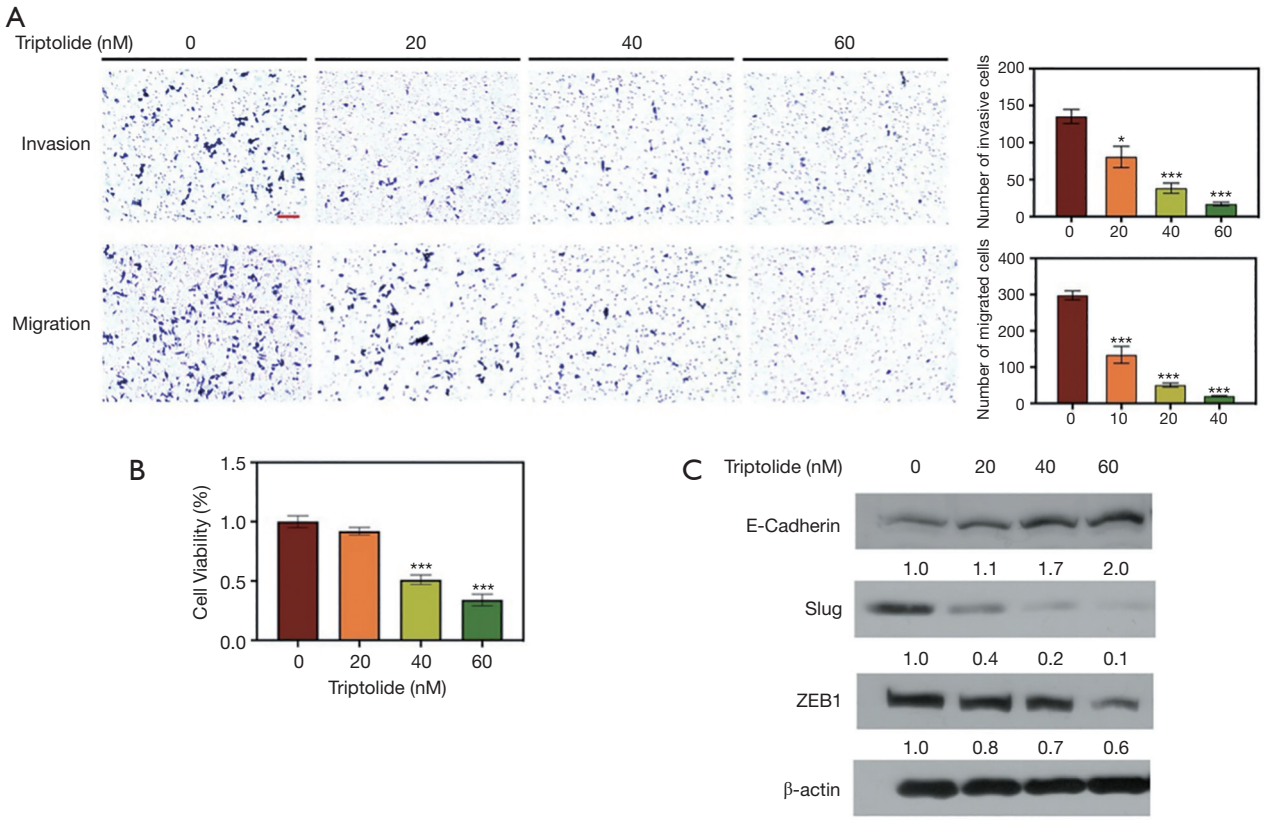

Figure 3 Triptolide reverses the EMT phenotype in A549/TaxR cells. (A) Migration and invasion of A549/TaxR cells as assessed by transwell assays after treatment with different doses of triptolide (0, 20, 40, and 60 nM) for 24 hours. (B) Cell viability after treatment with triptolide (0, 20, 40, and 60 nM) for 24 hours. (C) Expression levels of E-cadherin, Slug, and ZEB1 in A549/TaxR cells as evaluated by western blot after treatment with triptolide (0, 20, 40, and 60 nM) for 24 hours. Data are presented as the means ± SD. Scale Bar, 50 μm. *P<0.05, ***P<0.001 compared to controls. EMT, epithelial-mesenchymal transition; SD, standard deviation.

mean tumor volume of the vehicle group was 1,313 mm^3, while 948 and 638 mm^3 for the low-dose and high-dose triptolide groups, respectively. The body weight of mice was measured every day to identify any possible side effect of triptolide. No obvious weight loss was detected in triptolide-treated mice (*Figure 5C*), which indicates that triptolide did not induce significant systemic toxicity at the dosage applied.

IHC assay was performed in mice tumor samples to evaluate cell proliferation and apoptosis, and a significant decrease of PCNA expression as well as an increased percentage of TUNEL-positive apoptotic cells in the high-dose triptolide (0.8 mg/kg) group was demonstrated (*Figure 5D*). This means, that triptolide not only inhibited cell proliferation but also induced cell apoptosis in the A549/TaxR xenograft tumors *in vivo*.

Triptolide suppresses phosphorylation of GSK3 and p70S6K

Our results above showed that triptolide-induced downregulation of β-catenin inhibited the Wnt pathway. GSK-3, which has been found being inactivated through phosphorylation at serine 9/21 by protein kinase p70S6k, has been shown to be a negative regulator of β-catenin (27-29). To determine whether β-catenin degradation induced by triptolide was regulated by the dephosphorylation of GSK-3 and p70S6K in A549/TaxR cells, we examined the expression level of p-p70S6K, p-GSK-3α and p-GSK-3β. The downregulation of p-p70S6K, p-GSK-3α, and p-GSK-3β observed at increasing doses of triptolide is shown in *Figure 6A*; while down-regulation was clearly observed, a

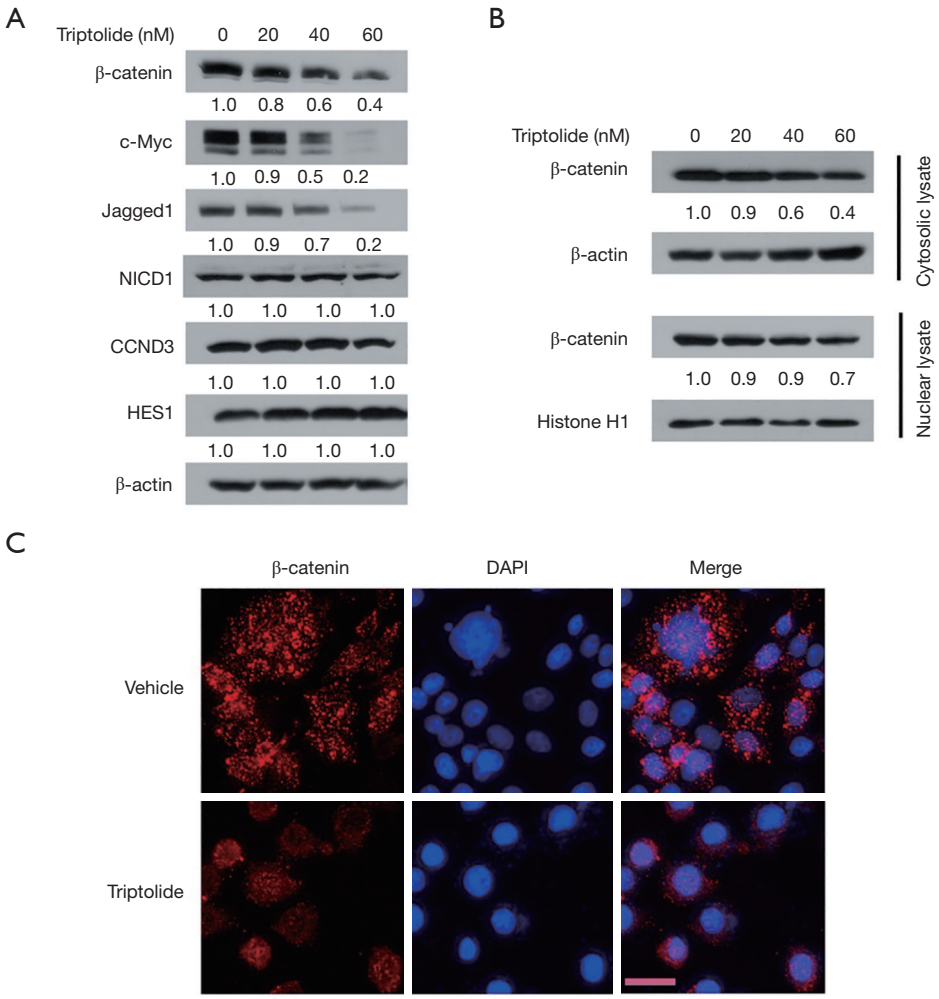

Figure 4 Triptolide reverses the EMT phenotype in A549/TaxR cells by repressing the Wnt/β-catenin pathway. (A) Expression of significant proteins involved in the Wnt and Notch signaling pathways in A549/TaxR cells after treatment with different concentrations of triptolide (0, 20, 40, and 60 nM) for 24 hours. (B) Levels of cytoplasmic and nuclear β-catenin in A549/TaxR cells after treatment with triptolide (0, 20, 40, and 60 nM) for 24 hours. (C) Expression of β-catenin in A549/TaxR cells as analyzed by IF after treatment with a vehicle and triptolide (60 nM) for 24 hours. Scale Bar, 50 μm. EMT, epithelial-mesenchymal transition; IF, immunofluorescence.

relationship between concentration of triptolide and total expression levels of p70S6K, GSK-3α, and GSK-3β could not be detected. Additionally, reductions of p-GSK-3α, p-GSK-3β and β-catenin were also found in mice tumor samples (*Figure 6B*). To conclude, triptolide suppressed the Wnt/β-catenin pathway by blocking the activity of p70S6K, and this activated GSK-3 to promote degradation of β-catenin.

Discussion

Triptolide induces apoptosis of many drug-resistant tumor cells, including vincristine-resistant KB cells, doxorubicin-resistant MES-SA cells, and adriamycin-resistant K562 cells (30). This study also found that vincristine-resistant KB cells and doxorubicin-resistant MES-SA cells were more sensitive to triptolide than their parental cells, which is similar to our findings that the IC50 value of triptolide in A549 cells is about 2 times higher than that in A549/TaxR cells. Considering these findings, triptolide may become a promising and broad-spectrum agent to treat chemoresistant cancers, but the mechanisms on how triptolide inhibits these cells still needs further investigation.

Our findings revealed that triptolide may act on the

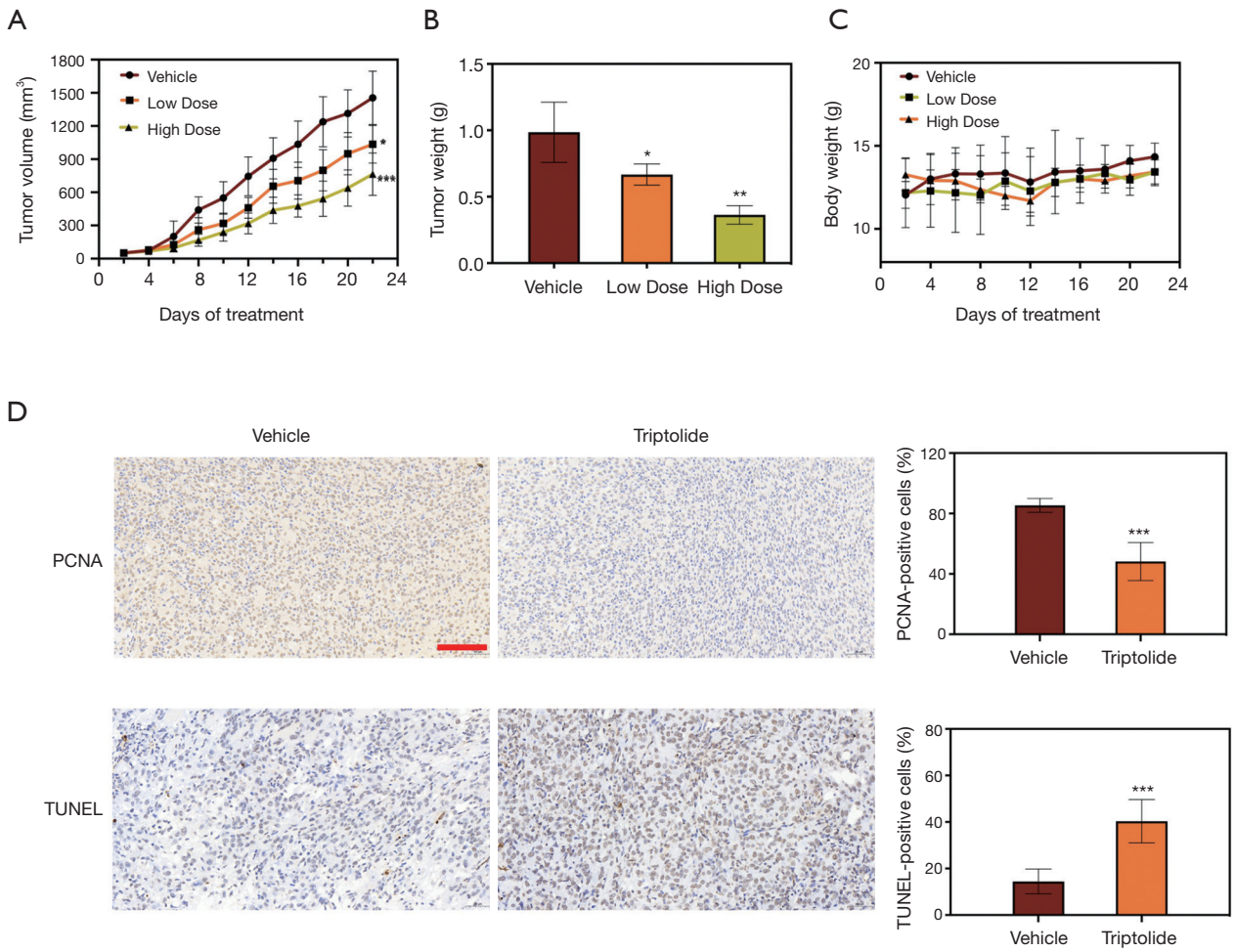

Figure 5 Anti-tumor effects of triptolide on mice A549/TaxR xenograft tumor in vivo. Mice received intraperitoneal injections every 2 days, and the experiment was terminated on day 20. (A) Anti-tumor effects of triptolide at low dose (0.4 mg/kg) and high dose (0.8 mg/kg). (B) Tumor weight of mice in all 3 groups on day 20. (C) Body weight of mice during the experiment. (D) Representative histological micrographs of PCNA and TUNEL as evaluated by H-score semi-quantitatively. PCNA was observed by immunohistochemistry assay and apoptosis of cells in mice tumor samples was detected by TUNEL staining, which were all evaluated by H-score semi-quantitatively later. Data are expressed as the means ± SD. Each experimental group included 5 mice. Scale bar, 100 μm. *P<0.05, **P<0.01, ***P<0.001 versus the vehicle group. PCNA, proliferating cell nuclear antigen; TUNEL, dUTP nick end labeling; SD, standard deviation.

mitochondrial apoptotic pathways by upregulating BAX, cleaved-PARP and cleaved-caspase 3, and downregulating Bcl-2, a major regulator of mitochondrial apoptotic pathways, and this led to death of A549/TaxR cells. In previous studies it was shown that death receptors and mitochondrial pathways are affected by triptolide, and apoptosis was induced in some solid and blood tumors (14,21,31). Besides, triptolide can also induce apoptosis mediated by apoptosis inducing factor (AIF) (32) and autophagic cell death (33).

The development of chemoresistance to cisplatin, taxol and epidermal growth factor receptor-tyrosine kinase inhibitors (EGFR-TKIs) is a major obstacle in the treatment of lung adenocarcinoma. EMT has been demonstrated as one of the mechanisms that contributes to chemoresistance such as to cisplatin (34-37) and has been reported to be either a cause or consequence of taxol-resistance in A549 cells (38). EMT has also been shown to cause acquired resistance to EGFR-TKIs such as erlotinib (39) and afatinib (40). This knowledge, combined with our present results showing that triptolide can reverse EMT, suggest that this molecule may be developed for the clinical treatment of drug-resistant

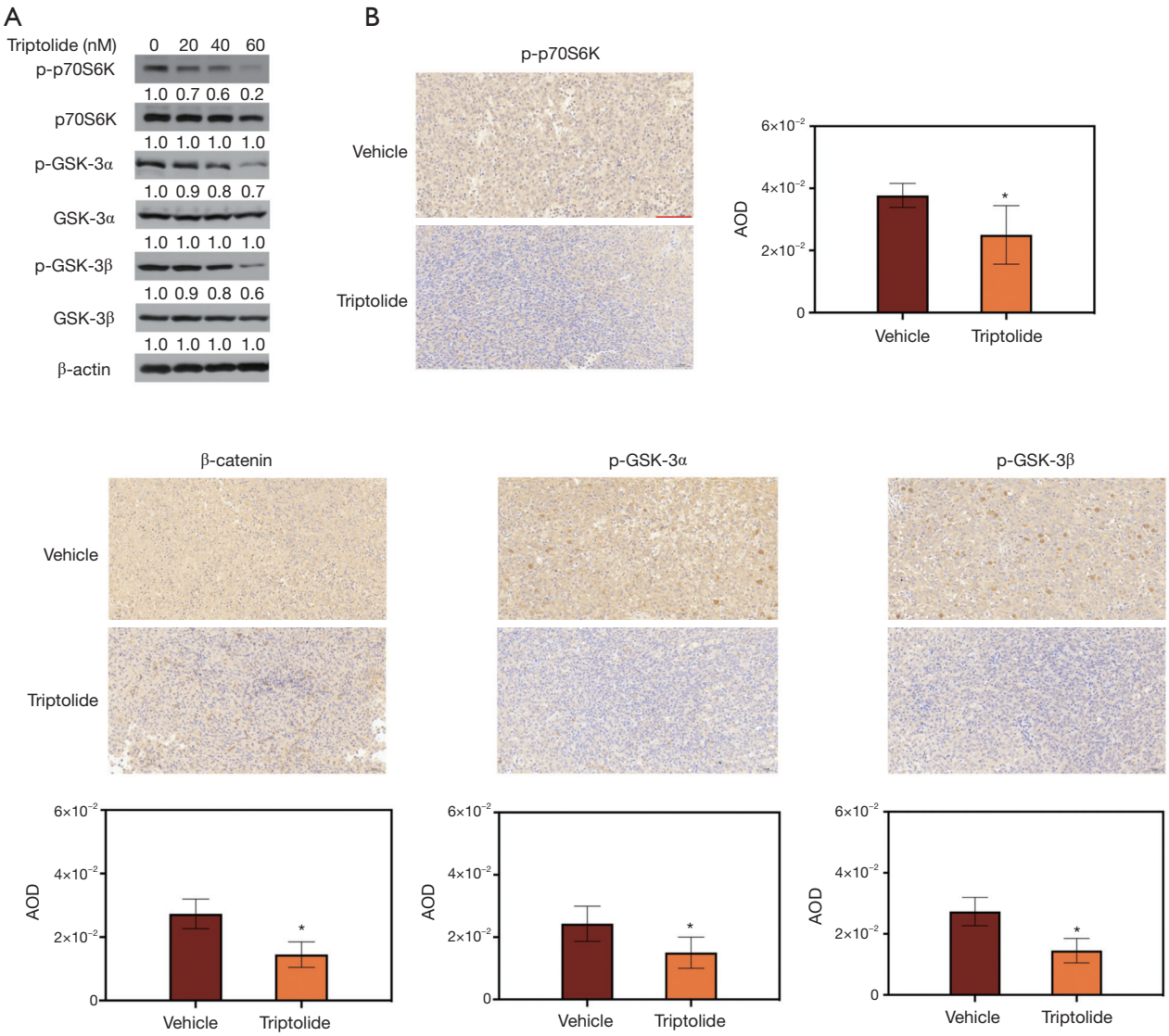

Figure 6 Triptolide suppresses the Wnt/β-catenin pathway by blocking phosphorylation of p70S6K and GSK3. (A) Expression level of p-p70S6K, total p70S6K, p-GSK-3α, total GSK-3α, p-GSK-3β, total GSK-3β and in A549/TaxR cells as detected by western blot after treatment with different doses of triptolide (0, 20, 40, and 60 nM). (B) Expression levels of p-p70S6K, p-GSK-3α, p-GSK-3β, and β-catenin in mice tumor samples as detected by IHC assay after treatment with a vehicle and high-dose triptolide (0.8 mg/kg). Scale bar, 100 μm. Staining of p-p70S6K, p-GSK-3α, p-GSK-3β, and β-catenin was evaluated by AOD = IOD/area semi-quantitatively. *P<0.05 *vs.* the vehicle group. IHC, immunohistochemistry; AOD, average optical density; IOD, integrated optical density.

cancers.

Inhibition of A549/TaxR xenografts by triptolide has been demonstrated by our experiments. However, due to the absence of taxol-treated mice bearing taxol-sensitive A549 tumors, the role of triptolide in breaking taxol resistance *in vivo* through EMT reversal is not yet proven and deserves further investigations.

EMT can be positively regulated by the Wnt/β-catenin pathway (26), a process in which GSK-3 plays a significant regulatory role. GSK-3 is found in all eukaryotes and is a widely-expressed and highly-conserved serine/threonine protein kinase that can be inactivated by p70S6k through phosphorylation at serine 9/21 (27-29). It is encoded by 2 genes which generate to 2 related proteins, GSK-3α and GSK-3β, in mammals. Active GSK-3β can prevent transcription of β-catenin target genes by stimulating

the degradation of β-catenin protein and promoting the destruction of nuclear phosphorylated β-catenin. Our results show that inhibition of the p70S6K/GSK-3/β-catenin signaling pathway is likely a major mechanism whereby triptolide inhibits EMT and the growth of A549/TaxR cells. However, the way triptolide inhibits the activity of p70S6K is not yet clear and requires further investigations.

In summary, our study demonstrated that triptolide, a natural product isolated from Tripterygium Wilfordii, induces apoptosis of A549/TaxR cells and reverses the EMT phenotype through repression of the p70S6K/GSK3/β-catenin signaling pathway, and suppresses the growth of A549/TaxR xenograft tumor without obvious toxicity *in vivo*. To our knowledge, this is the first study to proclaim triptolide's inhibition of EMT in taxol-resistant lung adenocarcinoma and associated mechanisms, moreover, these findings may provide a promising application for the combined therapeutic use of triptolide plus taxol, which could be applied for the treatment of chemoresistant lung adenocarcinoma.

Acknowledgments

The authors appreciate the academic support from AME Lung Cancer Collaborative Group.
Funding: This work was financially supported by the China National Science Foundation (81874396), Major Program of Shandong Province Natural Science Foundation (ZR2018ZC0232), Jinan Clinical Medicine Research Program for Thoracic Cancer (201912007), and a grant from the Special Construction Project Fund for Taishan Mountain Scholars of Shandong Province.

Footnote

Reporting Checklist: The authors have completed the ARRIVE reporting checklist. Available at http://dx.doi.org/10.21037/tlcr-21-145

Data Sharing Statement: Available at http://dx.doi.org/10.21037/tlcr-21-145

Conflicts of Interest: All authors have completed the ICMJE uniform disclosure form (available at http://dx.doi.org/10.21037/tlcr-21-145). HP serves as an unpaid Associate Editor (Controversies on Lung Cancer: Pros and Cons) of *Translational Lung Cancer Research* from Jul. 2019 to Jul. 2021. The other authors have no conflicts of interest to declare.

Ethical Statement: The authors are accountable for all aspects of the work in ensuring that questions related to the accuracy or integrity of any part of the work are appropriately investigated and resolved. Animal experiments were performed under a project license (No. 81874396) granted by the Ethical Committee for Animal Experimentation of the Second Hospital of Shandong University, in compliance with institutional guidelines for the care and use of animals.

References

1. Gao S, Li N, Wang S, et al. Lung Cancer in People's Republic of China. J Thorac Oncol 2020;15:1567-76.
2. Siegel RL, Miller KD, Jemal A. Cancer statistics, 2020. CA Cancer J Clin 2020;70:7-30.
3. Navada S, Lai P, Schwartz AG, Kalemkerian GP. Temporal trends in small cell lung cancer: analysis of the national Surveillance Epidemiology and End-Results (SEER) database. J Clin Oncol 2006;24 suppl:384S.
4. Gottesman MM, Fojo T, Bates SE. Multidrug resistance in cancer: Role of ATP-dependent transporters. Nat Rev Cancer 2002;2:48-58.
5. Iwatsuki M, Mimori K, Yokobori T, et al. Epithelial-mesenchymal transition in cancer development and its clinical significance. Cancer Sci 2010;101:293-9.
6. Brabletz T, Kalluri R, Angela Nieto M, et al. EMT in cancer. Nat Rev Cancer 2018;18:128.
7. Zhu X, Chen L, Liu L, et al. EMT-Mediated Acquired EGFR-TKI Resistance in NSCLC: Mechanisms and Strategies. Front Oncol 2019;9:1044.
8. Shao H, Ma J, Guo T, et al. Triptolide induces apoptosis of breast cancer cells via a mechanism associated with the Wnt/beta-catenin signaling pathway. Exp Ther Med 2014;8:505-8.
9. Reno TA, Tong SW, Wu J, et al. The triptolide derivative

MRx102 inhibits Wnt pathway activation and has potent anti-tumor effects in lung cancer. BMC Cancer 2016;16:439.
10. Li F, Cui H, Jin X, et al. Triptolide inhibits epithelial-mesenchymal transition and induces apoptosis in gefitinib-resistant lung cancer cells. Oncol Rep 2020;43:1569-79.
11. Yuan S, Wang L, Chen X, et al. Triptolide inhibits the migration and invasion of human prostate cancer cells via Caveolin-1/CD147/MMPs pathway (vol 84, pg 1776, 2016). Biomed Pharmacother 2020;122:109782.
12. Li X, Lu Q, Xie W, et al. Anti-tumor effects of triptolide on angiogenesis and cell apoptosis in osteosarcoma cells by inducing autophagy via repressing Wnt/beta-Catenin signaling. Biochem Biophys Res Commun 2018;496:443-9.
13. Krosch TCK, Sangwan V, Banerjee S, et al. Triptolide-mediated cell death in neuroblastoma occurs by both apoptosis and autophagy pathways and results in inhibition of nuclear factor-kappa B activity. Am J Surg 2013;205:387-96.
14. Kong J, Wang L, Ren L, et al. Triptolide induces mitochondria-mediated apoptosis of Burkitt's lymphoma cell via deacetylation of GSK-3 beta by increased SIRT3 expression. Toxicol Appl Pharmacol 2018;342:1-13.
15. Jacobson BA, Chen EZ, Tang S, et al. Triptolide and its prodrug minnelide suppress Hsp70 and inhibit in vivo growth in a xenograft model of mesothelioma. Genes Cancer 2015;6:144-52.
16. Chen Z, Sangwan V, Banerjee S, et al. Triptolide sensitizes pancreatic cancer cells to TRAIL-induced activation of the death receptor pathway. Cancer Lett 2014;348:156-66.
17. Phillips PA, Dudeja V, McCarroll JA, et al. Triptolide induces pancreatic cancer cell death via inhibition of heat shock protein 70. Cancer Res 2007;67:9407-16.
18. Oliveira A, Beyer G, Chugh R, et al. Triptolide abrogates growth of colon cancer and induces cell cycle arrest by inhibiting transcriptional activation of E2F. Lab Invest 2015;95:648-59.
19. Li CJ, Chu CY, Huang LH, et al. Synergistic anticancer activity of triptolide combined with cisplatin enhances apoptosis in gastric cancer in vitro and in vivo. Cancer Letters 2012;319:203-13.
20. Yanchun M, Yi W, Lu W, et al. Triptolide prevents proliferation and migration of Esophageal Squamous Cell Cancer via MAPK/ERK signaling pathway. Eur J Pharmacol 2019;851:43-51.
21. Liu L, Li G, Li Q, et al. Triptolide induces apoptosis in human leukemia cells through caspase-3-mediated ROCK1 activation and MLC phosphorylation. Cell Death & Disease 2013;4:e941.
22. Clinical Trials Using Triptolide Analog. Available online: https://www.cancer.gov/about-cancer/treatment/clinical-trials/intervention/triptolide-analog
23. Vichai V, Kirtikara K. Sulforhodamine B colorimetric assay for cytotoxicity screening. Nat Protocols 2006;1:1112-6.
24. Zhang C, Hao Y, Wu L, et al. Curcumin induces apoptosis and inhibits angiogenesis in murine malignant mesothelioma. Int J Oncol 2018;53:2531-41.
25. Nardi I, Reno T, Yun X, et al. Triptolide inhibits Wnt signaling in NSCLC through upregulation of multiple Wnt inhibitory factors via epigenetic modifications to Histone H3. Int J Cancer 2018;143:2470-8.
26. Gonzalez DM, Medici D. Signaling mechanisms of the epithelial-mesenchymal transition. Science Signaling 2014;7:re8.
27. Stambolic V, Woodgett JR. Mitogen inactivation of glycogen-synthase kinase-3-beta in intact-cells via serine-9 phosphorylation. Biochem J 1994;303:701-4.
28. Sutherland C, Leighton IA, Cohen P. Inactivation of glycogen-synthase kinase-3-beta by phosphorylation - new kinase connections in insulin and growth-factor signaling. Biochem J 1993;296:15-9.
29. Sutherland C, Cohen P. The alpha-isoform of glycogen-synthase kinase-3 from rabbit skeletal-muscle is inactivated by P70 S6 kinase or map kinase-activated protein kinase-1 in-vitro. FEBS Lett 1994;338:37-42.
30. Yi JM, Huan XJ, Song SS, et al. Triptolide Induces Cell Killing in Multidrug-Resistant Tumor Cells via CDK7/RPB1 Rather than XPB or p44. Mol Cancer Ther 2016;15:1495-503.
31. Zhao X, Zhang Q, Chen L. Triptolide induces the cell apoptosis of osteosarcoma cells through the TRAIL pathway. Oncol Rep 2016;36:1499-505.
32. Chan SF, Chen YY, Lin JJ, et al. Triptolide induced cell death through apoptosis and autophagy in murine leukemia WEHI-3 cells in vitro and promoting immune responses in WEHI-3 generated leukemia mice in vivo. Environ Toxicol 2017;32:550-68.
33. Mujumdar N, Mackenzie TN, Dudeja V, et al. Triptolide Induces Cell Death in Pancreatic Cancer Cells by Apoptotic and Autophagic Pathways. Gastroenterology 2010;139:598-608.
34. Zheng X, Carstens JL, Kim J, et al. Epithelial-to-mesenchymal transition is dispensable for metastasis but induces chemoresistance in pancreatic cancer. Nature

2015;527:525.
35. Fischer KR, Durrans A, Lee S, et al. Epithelial-to-mesenchymal transition is not required for lung metastasis but contributes to chemoresistance. Nature 2015;527:472.
36. Poh ME, Liam CK, Mun KS, et al. Epithelial-to-mesenchymal transition (EMT) to sarcoma in recurrent lung adenosquamous carcinoma following adjuvant chemotherapy. Thorac Cancer 2019;10:1841-5.
37. Marcucci F, Stassi G, De Maria R. Epithelial-mesenchymal transition: a new target in anticancer drug discovery. Nat Rev Drug Discov 2016;15:311-25.
38. Thomson S, Buck E, Petti F, et al. Epithelial to mesenchymal transition is a determinant of sensitivity of non-small-cell lung carcinoma cell lines and xenografts to epidermal growth factor receptor inhibition. Cancer Res 2005;65:9455-62.
39. Han ML, Zhao YF, Tan CH, et al. Cathepsin L upregulation-induced EMT phenotype is associated with the acquisition of cisplatin or paclitaxel resistance in A549 cells. Acta Pharmacologica Sinica 2016;37:1606-22.
40. Poh ME, Liam CK, Rajadurai P, et al. Epithelial-to-mesenchymal transition (EMT) causing acquired resistance to afatinib in a patient with epidermal growth factor receptor (EGFR)-mutant lung adenocarcinoma. J Thorac Dis 2018;10:E560-3.

(English Language Editor: J. Jones)

Cite this article as: Tian Y, Li P, Xiao Z, Zhou J, Xue X, Jiang N, Peng C, Wu L, Tian H, Popper H, Poh ME, Marcucci F, Zhang C, Zhao X. Triptolide inhibits epithelial-mesenchymal transition phenotype through the p70S6k/GSK3/β-catenin signaling pathway in taxol-resistant human lung adenocarcinoma. Transl Lung Cancer Res 2021;10(2):1007-1019. doi: 10.21037/tlcr-21-145

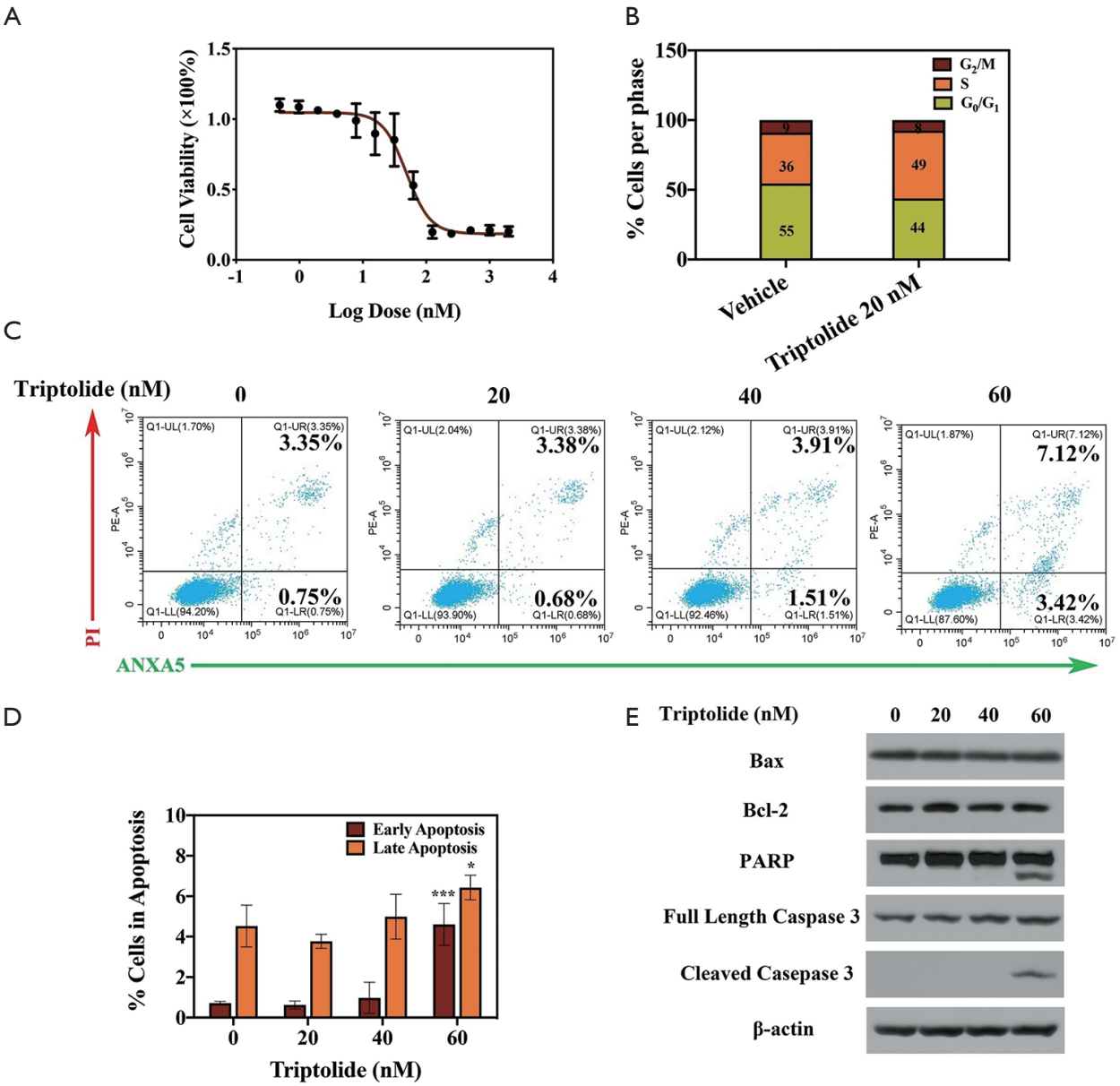

Figure S1 Triptolide inhibits proliferation and induces apoptosis of A549 cells. (A) Dose-dependent inhibition of the proliferation of A549 cells by triptolide. Cell viability was determined by SRB assay after treatment with triptolide for 72 hours. (B) S-phase arrest in A549 cells after treatment with triptolide (20 nM) for 24 hours. (C) Representative flow cytometric graphs of A549 cells after treatment with triptolide (0, 20, 40, and 60 nM) for 24 hours. (D) Quantification of apoptotic cells after treatment with triptolide. The graph shows AV-PI positive cells, and the data are presented as the means ± SD. (E) Expression levels of PARP, Caspase-3, Bcl-2, and Bax in A549 cells which were detected by western blot after treatment with triptolide for 24 hours. *P<0.05, ***P<0.001 compared to controls. SRB, sulforhodamine B; AV-PI, annexin V-propidium iodide; SD, standard deviation.

http://dx.doi.org/10.21037/tlcr-21-145